

**Ultrafast quasiparticle dynamics in the heavy-fermion compound YbRh<sub>2</sub>Si<sub>2</sub>**K. Kummer,<sup>1</sup> D. V. Vyalikh,<sup>2</sup> L. Rettig,<sup>3,4</sup> R. Cortés,<sup>3,5,\*</sup> Yu. Kucherenko,<sup>2,6</sup> C. Krellner,<sup>7</sup> C. Geibel,<sup>7</sup> U. Bovensiepen,<sup>3,4</sup> M. Wolf,<sup>3,5</sup> and S. L. Molodtsov<sup>8</sup><sup>1</sup>European Synchrotron Radiation Facility, 6 Rue Jules Horowitz, Boîte Postale 220, F-38043 Grenoble Cedex, France<sup>2</sup>Institut für Festkörperphysik, Technische Universität Dresden, D-01062 Dresden, Germany<sup>3</sup>Fachbereich Physik, Freie Universität Berlin, Arnimallee 14, D-14195 Berlin, Germany<sup>4</sup>Fakultät für Physik, Universität Duisburg-Essen, Lotharstrasse 1, D-47048 Duisburg, Germany<sup>5</sup>Abteilung Physikalische Chemie, Fritz-Haber-Institut der Max-Planck-Gesellschaft, Faradayweg 4-6, D-14195 Berlin, Germany<sup>6</sup>Institute for Metal Physics, National Academy of Sciences of Ukraine, UA-03142 Kiev, Ukraine<sup>7</sup>Max-Planck-Institut für Chemische Physik fester Stoffe, D-01187 Dresden, Germany<sup>8</sup>European XFEL GmbH, Albert-Einstein-Ring 19, D-22761 Hamburg, Germany

(Received 15 May 2012; revised manuscript received 16 August 2012; published 24 August 2012)

Understanding strongly correlated rare-earth intermetallic compounds requires knowledge of the nature of the fermionic quasiparticles in states near the Fermi level  $E_F$ . We report on a pump-probe experiment using femtosecond time- and angle-resolved photoemission spectroscopy to determine lifetimes of hot quasiparticles in the heavy-fermion compound YbRh<sub>2</sub>Si<sub>2</sub>. An unoccupied band with electronlike dispersion and a band bottom 0.2 eV above  $E_F$  was identified at  $\bar{\Gamma}$ , in agreement with band structure calculations for the subsurface region. Hot quasiparticle lifetimes from 30 to 80 fs were found for energies between 0.4 and 0.1 eV above  $E_F$ . These lifetimes generally follow the typical monotonous increase towards  $E_F$ , in agreement with earlier studies on Yb and Rh elemental metals. However, at normal emission the lifetimes at around 0.2 eV exceed this trend by about +20 fs. This difference decreases with increasing photoemission angle and can be assigned to the particular band that is probed in YbRh<sub>2</sub>Si<sub>2</sub>. Potential microscopic scenarios are discussed.

DOI: [10.1103/PhysRevB.86.085139](https://doi.org/10.1103/PhysRevB.86.085139)

PACS number(s): 78.47.J–, 71.27.+a, 71.20.–b

**I. INTRODUCTION**

Intermetallic systems containing elements with a partially filled  $4f$  or  $5f$  electron shell exhibit a wide range of exotic phenomena such as, e.g., valence fluctuations, quantum criticality, magnetic order competing with superconductivity, or heavy-fermion (HF) and Kondo behavior. The reason for this variety of phenomena has to be in the details of the electronic structures around the Fermi level  $E_F$ , which are intimately connected to the material properties. Hence a great deal of attention has been given to the similarities and peculiarities among the electronic structures of rare-earth intermetallics. The general difference to, for instance, transition-metal systems, characterized by  $dd$  correlations, is the presence of the very localized, almost atomiclike  $f$  electrons of the rare-earth ions. The interaction of these states with itinerant  $s$ ,  $p$ , or  $d$  states of the transition metals are thought to be behind many of the unusual material properties. In order to understand these interactions and the involved localized-itinerant duality of fermions in those systems a profound knowledge of their role in the electronic structure around  $E_F$  is needed.

Angle-resolved photoelectron spectroscopy (ARPES) probes the momentum-dependent electronic structure  $E(\mathbf{k})$  directly and can provide information on, for instance, effective masses of the electron quasiparticles. With the realization of pump-probe photoemission instruments further information has become accessible: the dynamics of excited quasiparticles down to femtosecond (fs) and even attosecond (as) time scales.<sup>1–3</sup> It has thus become possible to study elementary processes such as electron-electron or electron-phonon scattering with momentum resolution which has generated significant experimental input for a wide range of material classes. Among others, the quasiparticle dynamics at noble-metal surfaces,<sup>4</sup> in

two-dimensional films and charge-density wave materials,<sup>5</sup> and in high- $T_c$  superconductors<sup>6–8</sup> have been examined.

However, because of the imbalance in the occupation of states below and above  $E_F$  at sensible pump fluences it is not trivial to study the dynamics of excited states with pump-probe photoemission, especially closely above  $E_F$ . Typically this problem is approached by means of two-photon photoemission (2PPE) where the photon energies of the pump and probe pulse are limited to  $\Phi/2 < \hbar\omega < \Phi$ , with  $\Phi$  the material's work function.<sup>2,3</sup> This prohibits direct photoemission from the occupied electronic states below  $E_F$  due to absorption of a single photon and only the desired information about the excited, previously unoccupied states enters the photoemission spectrum. However, standard 2PPE puts severe limitations on the usable photon energy range for both the pump and the probe beam. As a result, not all desired excitations may be applicable. Vice versa, 2PPE is not compatible with high-photon energy probe pulses in the extended ultraviolet (XUV) and soft x-ray range as provided by high-harmonic generation (HHG) or free electron laser sources. But, in particular, for transition-metal and rare-earth compounds it is highly desirable to go to higher photon energies. The interesting correlation effects found in these materials are mainly due to the  $d$  and  $f$  states which show notable photoemission cross sections only in the XUV range. Appropriate schemes for time-resolved photoemission at these energies are currently developed.<sup>9,10</sup>

We performed pump-probe photoemission experiments on the HF compound YbRh<sub>2</sub>Si<sub>2</sub> using infrared (IR) pump and ultraviolet (UV) probe pulses with a photon energy above  $\Phi$ . YbRh<sub>2</sub>Si<sub>2</sub> has been one of the most intensively studied rare-earth compounds since the discovery of a quantum critical point in its phase diagram. It is characterized by a complex

interplay of the localized  $4f$  states of Yb and itinerant valence states of Rh at  $E_F$ .<sup>11–13</sup> The Yb ions in  $\text{YbRh}_2\text{Si}_2$  are intermediate valent, but close to the trivalent,  $4f^{13}$  electron configuration.<sup>14</sup> The  $4f^{14}$  levels are only partly populated. In selected regions of the Brillouin zone (BZ), those levels are pushed above  $E_F$  by few meV due to the hybridization with valence bands. Unfortunately, this cannot be studied directly with pump-probe photoemission because the region a few meV above  $E_F$  is dominated by the hot electron gas created during the pump process. It was, however, possible to look at their antagonists, the Rh valence bands that take part in the formation of heavy  $4f$  bands. Here we report hot electron lifetimes in excited valence band states closely above  $E_F$ . In particular, we found notably extended quasiparticle lifetimes around the  $\Gamma$  point of the Brillouin zone where heavy  $4f$  bands have been found previously.<sup>12</sup>

## II. EXPERIMENTAL DETAILS

For the time-resolved ARPES (trARPES) measurements an amplified Ti:sapphire laser system operating at 300 kHz repetition rate and an ultrahigh vacuum system equipped with an electron time-of-flight (TOF) spectrometer were combined. The femtosecond laser pulses were used to optically excite (pump) the samples and to subsequently probe the pump-induced change of the electron distribution. The employed experimental setup is described elsewhere.<sup>5,15</sup> In the present experiment, the pump beam was generated by an optical parametric amplifier (OPA) operating in the IR and the photon energy was set to 0.95 eV. We used incident pump fluences of  $100 \mu\text{J}/\text{cm}^2$ . The probe beam was generated by quadrupling of the fundamental output of a Ti:sapphire amplifier which provides femtosecond pulses at 6.0 eV. The delay between pump and probe beam can be adjusted with an optical delay stage.

The overall time resolution was determined by fitting a Gaussian to the pump-probe cross correlation (XC), yielding 70–80 fs full width at half maximum. A TOF spectrometer with an acceptance angle of  $3^\circ$ , corresponding to a momentum resolution of about  $0.05 \text{ \AA}^{-1}$ , and an energy resolution of 10 meV at 2 eV kinetic energy was used for photoelectron detection. To obtain angular resolved spectra the sample was

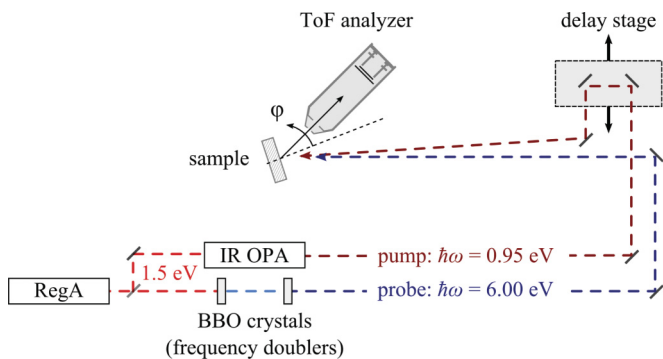


FIG. 1. (Color online) Scheme of the experimental setup. A tabletop laser setup was used to generate the ultrashort IR pump and UV probe pulses. It was connected to a UHV chamber equipped with a TOF electron energy analyzer for photoemission spectroscopy.

gradually rotated around the axis in the sample surface plane in order to measure off-normal emission. A scheme of the experimental setup is shown in Fig. 1. The single-crystal samples were cleaved *in situ* in ultrahigh vacuum with a base pressure  $p < 10^{-10}$  mbar at  $T = 30 \text{ K}$  and kept at this temperature during the measurements. Excellent crystal quality has already been demonstrated in a number of previous ARPES experiments.<sup>12,13</sup> The work function was found to be about 4.0 eV.

## III. EXPERIMENTAL RESULTS

Figure 2 shows ARPES spectra taken for a series of emission angles around normal emission with the pump-probe delay fixed at  $\Delta t = 50 \text{ fs}$ . Several bandlike features can be distinguished both in the logarithmic and the linear plot which disperse as one moves away from  $\Gamma$ , the center of the surface Brillouin zone: Two holelike bands, (1) and (2), with their band tops at about 0.7 and 0.5 eV below  $E_F$ , are visible

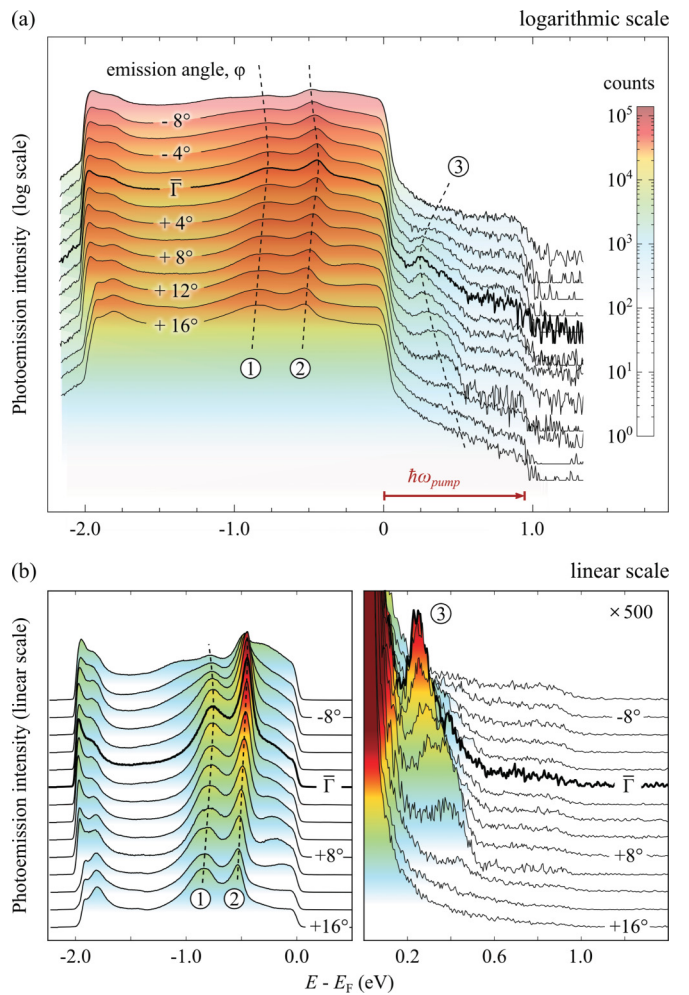


FIG. 2. (Color online) (a) Logarithmic and (b) linear scale plot of the angle-resolved photoemission from electronic states below and above  $E_F$  in  $\text{YbRh}_2\text{Si}_2$ . The spectra were taken with 6 eV probe pulses 50 fs after excitation with infrared laser pulses of 0.95 eV energy. Two dispersing holelike states are visible below  $E_F$  [(1), (2)]. One electronlike state emerges above  $E_F$  (3) from the featureless background of hot electrons between  $E_F$  and 0.95 eV.

in the probed occupied electronic structure between  $E_F$  and  $E - E_F = -2$  eV, where the low-energy cutoff of the spectra sets in. Above  $E_F$ , between 0 and 0.95 eV energy, a population of hot electrons is built up by the optical excitation with the IR pump pulse. In this energy range a third, electronlike dispersing band, (3), is detected with the band bottom at 0.2 eV above  $E_F$ . This photoemission feature persists even for  $\Delta t > 100$  fs and its energy position relative to  $E_F$  does not change with the pump photon energy. Hence it is not due to photoemission from occupied states with  $(\hbar\omega_{\text{IR}} + \hbar\omega_{\text{UV}})$  via virtual intermediate states which can occur when the pump and probe beam temporally overlap. Instead, it reflects a part of the unoccupied band structure that was populated by the optical excitation.

The observed occupied band structure is very different from ARPES data obtained with synchrotron light in the photon energy range from 45 to 110 eV.<sup>11</sup> This is due to the very different photoemission cross sections in the XUV and at 6 eV photon energy. In the XUV one is most sensitive to states with  $d$  and  $f$  orbital character while states with lower angular momentum character dominate spectra taken in the near-optical range.<sup>16</sup> In particular, contributions of Yb  $4f$  states become very weak below 20 eV photon energy.<sup>17,18</sup> Figure 3 shows the evolution of the Yb  $4f_{7/2}$  intensity at  $E_F$  in YbRh<sub>2</sub>Si<sub>2</sub> as the photon energy is gradually decreased from 40 eV down to 6 eV. With the UV laser pulses the  $4f$  peak is hardly distinguishable. Very recently a photoemission experiment on YbRh<sub>2</sub>Si<sub>2</sub> was reported where a laser source operating at 7 eV photon energy had been used.<sup>19</sup> Despite the very low photoemission cross section the  $4f_{7/2}$  states at  $\bar{\Gamma}$  came out clearly. Note that this experiment had been done with a very-high-energy resolution of only 3 meV which allows to better separate the sharp  $4f$  states from the Rh surface band

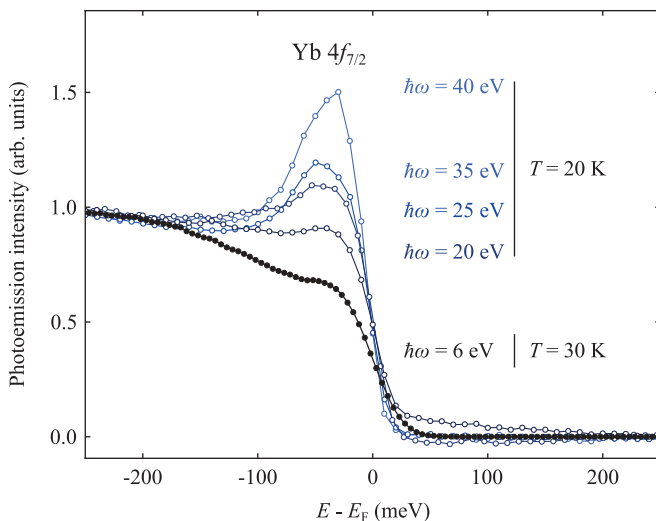


FIG. 3. (Color online) Photon energy dependence of the  $4f_{7/2}$  contribution in YbRh<sub>2</sub>Si<sub>2</sub> around  $\bar{\Gamma}$  between 40 and 6 eV photon energy. The data between 40 and 20 eV (open circles) were recorded at beamline UE112 PGM-2 at BESSY using the 1<sup>2</sup> endstation with the sample kept at  $T = 20$  K. The 6 eV curve (solid circles) is the data taken with the trARPES laser setup and with the sample temperature being  $T = 30$  K. The intensities have been normalized to the value at  $-250$  meV.

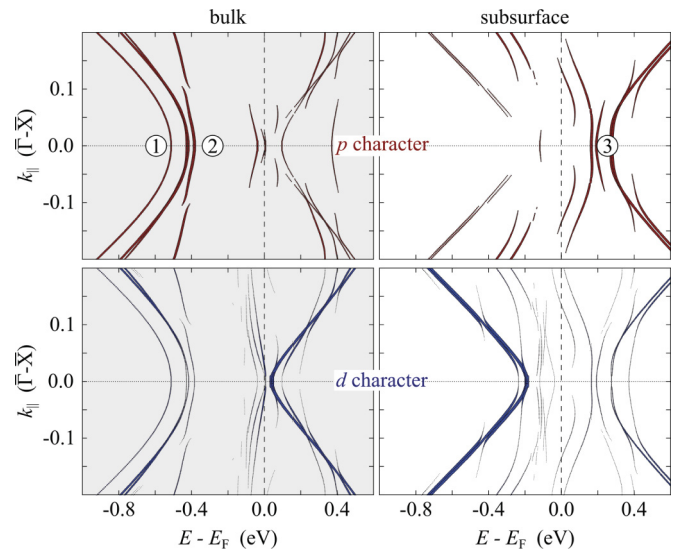


FIG. 4. (Color online) Calculated Rh  $p$  and  $d$  character of electron bands in the YbRh<sub>2</sub>Si<sub>2</sub> slab consisting of 15 atomic layers. Only partial contributions with weights  $c_i(k) > 0.01$  are shown.

approaching them.<sup>12</sup> We cannot achieve that with our pump-probe setup because of the lower-energy resolution of our TOF detector and the large spectral bandwidth of the fs laser pulses which are both of the order of  $\Delta E = O(10$  meV). Also note that we cannot estimate to which extent Yb-terminated surface regions are also covered by the beam spot. In that case, a rather broad Yb  $4f_{7/2}$  peak at  $-0.7$  eV is observed at higher photon energies<sup>20</sup> which could not be separated from valence band photoemission at low photon energies.

To assign the dispersive features (1)–(3) we performed full-relativistic band structure calculations for a slab modeling the YbRh<sub>2</sub>Si<sub>2</sub> crystal. They allow to determine the symmetry of the bands as well as to discriminate between their surface and bulk origin. Details of the calculations are described elsewhere,<sup>11</sup> but this time Yb  $4f$  states were taken into account in the valence basis set. The results are shown in Fig. 4 for the relevant region around  $\bar{\Gamma}$  and assuming a Si terminated surface. Reasonable agreement with the experimental data for the regions below and above  $E_F$  is found when considering both subsurface and bulk bands with  $p$  symmetry (upper two panels of Fig. 4). For the energy region between 0.2 and 0.4 eV the calculations suggest the presence of multiple bands whereas only one peak is seen in the experimental data. It may be possible that more than one band contributes to the experimentally observed state above  $E_F$ . Note that the energy positions of experimentally observed and calculated bands do not necessarily coincide, in particular where  $4f$  and valence states interact. The  $p$  bands above  $E_F$  might be closer together than the calculations suggest.

As mentioned above, the dispersive band (3) remains visible in the spectra even for pump-probe delays  $\Delta t > 100$  fs, which is far longer than the combined temporal width of pump and probe pulse. This enabled us to study the dynamics of the quasiparticles close to  $E_F$  as a function of electron momentum. To this end, we varied the angle between surface normal and detector from  $0^\circ$  ( $\bar{\Gamma}$ ) gradually to higher emission angles and measured the photoemission spectra as a function of  $\Delta t$ . The

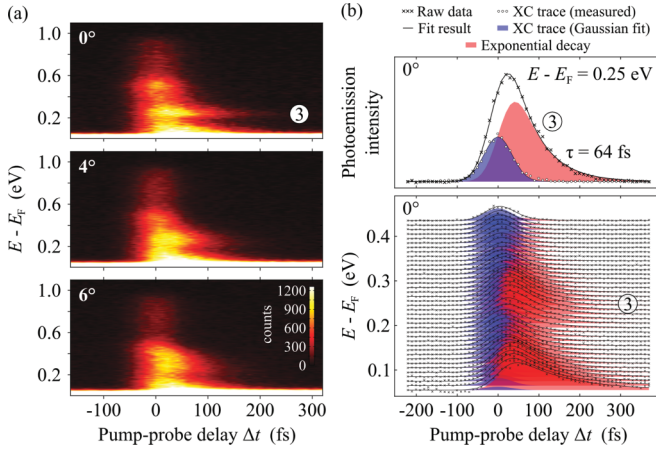


FIG. 5. (Color online) (a) Photoelectron intensity above  $E_F$  as a function of pump-probe delay at the  $\bar{\Gamma}$  point as well as  $4^\circ$  and  $6^\circ$  off normal emission. (b) The time-dependent intensity was fitted with two components modeling the zero lifetime background and the exponentially decaying electron population (upper panel). The analysis was performed for a wide ( $E - E_F$ ) range divided into 10 meV narrow slices (lower panel).

obtained time-dependent photoemission intensities are shown as color maps in Fig. 5(a) for different emission angles.

The topmost map in Fig. 5(a) was measured at  $\bar{\Gamma}$ . A clear signature of band (3) is visible at 0.2 eV and a quasiparticle population up to about  $\Delta t = 200$  fs is identified. This signal of band (3) is observed on top of a background close to  $E_F$  (see Fig. 1). When going to off-normal emission [Fig. 5(a), middle and lower panel], band (3) starts to overlap with the virtual image of the occupied band (2) due to the electronlike and holelike dispersion of the two features, respectively. This and a loss in intensity and contrast prevent the separation of band (3) from the background for emission angles higher than  $\sim 6^\circ$ . Therefore, we restrict our analysis to small  $k_{\parallel}$  values.

The energy-dependent lifetimes  $\tau(E)$  of the electron population above  $E_F$  were determined by analyzing the time-dependent population in Fig. 5(a) within separate energy intervals of 10 meV width each. For the fit analysis we assumed two components, as shown in the upper panel of Fig. 5(b): a Gaussian approximation to the pump-probe cross correlation and a single exponential decay, convolved with the XC. The Gaussian component accounts for the intensity which forms the background for feature (3) in Fig. 1. This contribution is symmetric around  $\Delta t = 0$  fs and reflects photoemission from occupied states via virtual intermediate states due to simultaneous absorption of both an IR and an UV photon. It dominates the intensity between 0.8 and 1.0 eV and was used to determine the cross correlation (XC) between pump and probe pulse. We obtain typical values for the XC width of 70–80 fs. Our interpretation of this intensity is supported (i) by the cutoff at  $E - E_F = 0.95$  eV, which reflects the Fermi edge, and (ii) by the feature near 0.45 eV, which is exactly 0.95 eV above band (2). The second contribution accounts for the hot electron population and we use a single exponential decay convolved with the XC. In this case, the exponential time constant reflects the hot electron lifetimes. Both contributions are shown in Fig. 5(b), together with the experimental data they shall describe. Note that for  $E - E_F$  larger than  $\sim 0.45$  eV the

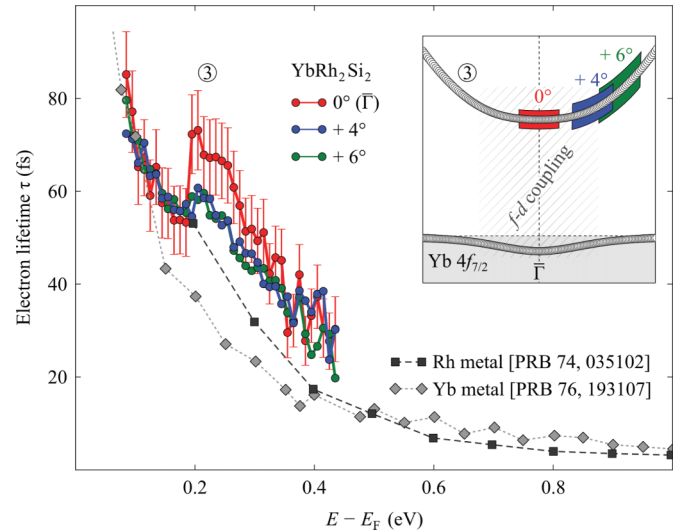


FIG. 6. (Color online) Electron lifetime vs energy distance to  $E_F$  for the pumped electron population at normal emission ( $\bar{\Gamma}$ ) as well as  $4^\circ$  and  $6^\circ$  off normal emission. As a reference we show published previously data for Rh and Yb metal (Refs. 21 and 22). The inset shows a simplified two-level hybridization model illustrating the coupling between valence and 4f states in YbRh<sub>2</sub>Si<sub>2</sub>. The red, blue, and green boxes denote the  $k$  intervals probed at  $0^\circ$ ,  $4^\circ$ , and  $6^\circ$  emission angle, respectively.

electron population became too low to give meaningful fit results.

The lifetimes which we obtained at the different emission angles for  $0.08$  eV  $< E - E_F < 0.42$  eV are shown in Fig. 6 together with data previously published for Rh metal<sup>21</sup> and Yb metal.<sup>22</sup> As a general trend, our data show decreasing quasiparticle lifetimes with increasing energy above  $E_F$ , as the Fermi liquid theory (FLT) predicts.<sup>23</sup> However, at  $\bar{\Gamma}$  and at the energies of band (3) a sudden jump in the electron lifetime occurs which deviates from the FLT prediction and from lifetimes observed in Yb or Rh. When going away from  $\bar{\Gamma}$  this deviation is reduced and the behavior resembles more the behavior found for the simple metals.

#### IV. DISCUSSION

It has already been known from studies of Yb and Rh elemental metals that electron-electron scattering involving 4f and 4d electrons leads to deviations in quasiparticle lifetimes from the FLT predictions.<sup>21,22</sup> However, the observation was still monotonously increasing hot electron lifetimes towards  $E_F$ , in contrast to what we observe here between 0.2 and 0.4 eV. Compared to elemental Yb or Rh metal, YbRh<sub>2</sub>Si<sub>2</sub> is a rather nontrivial material characterized by a complex electronic structure and strong electron correlations. In this light, several scenarios can be conceived which could explain our observations.

First, with increasing energy ( $E - E_F$ ) a new band is reached at  $\sim 0.2$  eV. The new band can certainly have a different self-energy than the electrons probed between  $E_F$  and the band bottom, possibly leading to the peculiar dependence of  $\tau(E)$ . On the other hand, an electronic intraband scattering process such as observed before in image potential states

on noble-metal surfaces<sup>24</sup> could be responsible. Intraband scattering towards the band bottom would lead to a delayed population of states at  $\bar{\Gamma}$ . This could also explain the angular dependence of the lifetimes. A delayed population above  $E_F$  could also built up by the decay of holes generated during the optical excitation, e.g., in the bands 0.5 and 0.7 eV below  $E_F$ . Such processes were discussed to explain results on Cu(111) which resemble the ones reported in Fig. 6.<sup>25</sup> However, in Cu the peak in emission intensity fell together in energy with a lifetime minimum, and the jump in quasiparticle lifetimes was observed at higher intermediate state energies, where the photoemission intensity has already died down. Moreover, the dynamics reported there are the average over a large part of the BZ and where also observed in polycrystalline Cu samples.<sup>26</sup> Both is very different to our data, where the sudden jump in the quasiparticle lifetimes is seen at a maximum in photoemission intensity and related to a particular  $k_{\parallel}$ . Transient excitonic states may explain our data, too. The photon energy 0.95 eV used for the optical excitation meets the energy separation between the occupied band (1) and band (3) at  $\bar{\Gamma}$ . Thus direct optical transitions, transferring an electron into (3) and leaving a hole in (1) behind, could be possible. With the electron and hole already in the respective potential minima, a transient excitonic state with a different lifetime may form at  $\bar{\Gamma}$ .<sup>27</sup> But transient excitonic states in metals are thought to exist only on very short time scales, significantly shorter than those discussed here, because of the almost instantaneous buildup of a screening charge cloud.<sup>28</sup> On the other hand, scattering involving phonons (or other bosons) is known to occur on much slower time scales than the ones reported here (picoseconds instead of femtoseconds—see, for instance, Refs. 6, 15, and 29). We can therefore exclude the significance of such processes for our experimental findings.

Another potential scenario involves the Yb  $4f_{7/2}$  states at  $E_F$  in YbRh<sub>2</sub>Si<sub>2</sub>. It is known that valence states close to  $E_F$  can be subject to hybridization with the atomiclike, localized  $4f$  states.<sup>11–13</sup> Our full-relativistic calculations show that band (3) is to couple to the Yb  $4f_{7/2}$  levels at  $E_F$  due to their similar symmetries. This is sketched with a simple two-level model in the inset of Fig. 6. Hybridization between band (3) and the  $4f_{7/2}$  states at  $\bar{\Gamma}$  would induce an electronlike dispersion of the  $4f$  level, which indeed was observed previously.<sup>12</sup> One can speculate that this hybridization will lead to a stronger localization of the involved valence states, reducing the scattering rate with the sea of itinerant electrons. In recent *ab initio*  $GW + T$  calculations on Yb metal the inclusion of interacting valence  $4f$  states resulted in significantly larger quasiparticle lifetimes than when the  $4f$  states were treated as core states.<sup>22</sup> Furthermore, from conventional ARPES it can already be anticipated that hybridization to  $f$  states leads to extended quasiparticle lifetimes, because the natural linewidth of the respective spectral features is considerably narrower than that of other valence band features. The effect of hybridization on the  $4f$  levels has already been studied in great detail with conventional ARPES. Deviating from the behavior of noninteracting  $4f$  states, bandlike dispersion, and level crossings of the crystal field split states were found.<sup>12</sup> Much less is known about the effect of hybridization on the valence states that take part in the formation of heavy bands. If the hybridization scenario is responsible for the experimental observations, interesting

perspectives for further studies of the detailed mechanisms and consequences of the interaction of localized and itinerant electronic states will open up. In particular, experimental insight into how exactly HF behavior is reflected in the dynamics of the involved quasiparticles can be gained.

On the basis of the present data, we cannot make definite claims which of the proposed scenarios is responsible for the extended quasiparticle lifetimes at  $\bar{\Gamma}$ . For instance, delayed electron populations have been observed before and successfully modeled by using simple rate equations.<sup>30</sup> We repeated the fit analysis shown in Fig. 5(b) by using an appropriate set of rate equations instead of a single experimental decay and obtained a similarly good agreement with the data. Hence a delayed population of the states lies well within the scope of the data presently at hand. Further experimental efforts are needed to exclude or substantiate some of the proposed scenarios. For instance, one can repeat the measurements at different pump beam energies. If the behavior found at 0.95 eV vanished at higher photon energies, that would support the scenario involving excitonic states. Other scenarios, on the other hand, shall not depend much on the particular excitation energy. Using a two-dimensional channel plate detector one could follow the dynamics of the electron population in different parts of the Brillouin zone at the same time, which would allow to identify intraband scattering processes.

The correlation of hybridization to localized Yb  $4f$  states at  $E_F$  and the extended quasiparticle lifetimes in band (3) could be verified by demonstrating a high  $f$  character contribution to band (3) at  $\bar{\Gamma}$ . Such a contribution is a signature of hybridization to the  $4f$  levels. To do that one has to go to higher probe beam energies in the XUV range, to 110 eV, where photoemission from states with no  $f$  orbital character is suppressed.<sup>31</sup> This photon energy range is becoming more and more accessible for trARPES experiments with the currently developed HHG laser sources. Note that the experiment reported here has been conducted in a nonstandard scheme, with  $\hbar\omega > \Phi$ , that is readily transferable to high probe photon energies.

## V. SUMMARY

A dispersing, subsurface state with the band bottom at  $\bar{\Gamma}$  and only 0.2 eV above  $E_F$  was found in YbRh<sub>2</sub>Si<sub>2</sub> by means of pump-probe photoemission. At  $\bar{\Gamma}$ , the lifetimes of excited quasiparticles that can be assigned to this band notably stand out from those found for other excited hot electrons and those reported in previous studies of Yb and Rh metal. These differences decrease when going away from  $\bar{\Gamma}$ . Several microscopic scenarios that could explain our observations were discussed, also in light of potential further experimental studies. From the point of view of heavy-fermion physics, it will be particularly attractive if the extended quasiparticle lifetimes in the valence state can be unambiguously related to interaction with the  $4f$  levels at  $E_F$  and the resulting formation of heavy bands.

## ACKNOWLEDGMENTS

This work was supported by the DFG (Grants No. VY64/1-1, No. GE602/2-1, and No. BO 1832/2-2). R.C. acknowledges support from the Alexander von Humboldt Foundation.

- \*Present address: Brookhaven National Laboratory, Upton, NY 11973.
- <sup>1</sup>A. L. Cavalieri, N. Müller, Th. Uphues, V. S. Yakovlev, A. Baltuka, B. Horvath, B. Schmidt, L. Blümel, R. Holzwarth, S. Hendel, M. Drescher, U. Kleineberg, P. M. Echenique, R. Kienberger, F. Krausz, and U. Heinzmann, *Nature (London)* **449**, 1029 (2007).
  - <sup>2</sup>H. Petek and S. Ogawa, *Prog. Surf. Sci.* **56**, 239 (1997).
  - <sup>3</sup>M. Weinelt, *J. Phys.: Condens. Matter* **14**, R1099 (2002).
  - <sup>4</sup>P. M. Echenique, R. Berndt, E. V. Chulkov, Th. Fauster, A. Goldmann, and U. Höfer, *Surf. Sci. Rep.* **52**, 219 (2004).
  - <sup>5</sup>U. Bovensiepen and P. S. Kirchmann, *Laser Photon. Rev.* (2012), doi: [10.1002/lpor.201000035](https://doi.org/10.1002/lpor.201000035).
  - <sup>6</sup>R. Cortés, L. Rettig, Y. Yoshida, H. Eisaki, M. Wolf, and U. Bovensiepen, *Phys. Rev. Lett.* **107**, 097002 (2011).
  - <sup>7</sup>J. Graf, C. Jozwiak, C. L. Smallwood, H. Eisaki, R. A. Kaindl, D.-H. Lee, and A. Lanzara, *Nat. Phys.* **7**, 805 (2011).
  - <sup>8</sup>L. Rettig, R. Cortés, S. Thirupathiah, P. Gegenwart, H. S. Jeevan, M. Wolf, J. Fink, and U. Bovensiepen, *Phys. Rev. Lett.* **108**, 097002 (2012).
  - <sup>9</sup>T. Haarlammer and H. Zacharias, *Curr. Op. Solid State Mater. Sci.* **13**, 13 (2009).
  - <sup>10</sup>S. Hellmann, M. Beye, C. Sohrt, T. Rohwer, F. Sorgenfrei, H. Redlin, M. Kalläne, M. Marczyński-Bühlow, F. Hennies, M. Bauer, A. Föhlisch, L. Kipp, W. Wurth, and K. Rossnagel, *Phys. Rev. Lett.* **105**, 187401 (2010).
  - <sup>11</sup>D. V. Vyalikh, S. Danzenbächer, Yu. Kucherenko, C. Krellner, C. Geibel, C. Laubschat, M. Shi, L. Patthey, R. Follath, and S. L. Molodtsov, *Phys. Rev. Lett.* **103**, 137601 (2009).
  - <sup>12</sup>D. V. Vyalikh, S. Danzenbächer, Yu. Kucherenko, K. Kummer, C. Krellner, C. Geibel, M. G. Holder, T. K. Kim, C. Laubschat, M. Shi, L. Patthey, R. Follath, and S. L. Molodtsov, *Phys. Rev. Lett.* **105**, 237601 (2010).
  - <sup>13</sup>S. Danzenbächer, D. V. Vyalikh, K. Kummer, C. Krellner, M. Holder, M. Höppner, Yu. Kucherenko, C. Geibel, M. Shi, L. Patthey, S. L. Molodtsov, and C. Laubschat, *Phys. Rev. Lett.* **107**, 267601 (2011).
  - <sup>14</sup>K. Kummer, Yu. Kucherenko, S. Danzenbächer, C. Krellner, C. Geibel, M. G. Holder, L. V. Bekenov, T. Muro, Y. Kato, T. Kinoshita, S. Huotari, L. Simonelli, S. L. Molodtsov, C. Laubschat, and D. V. Vyalikh, *Phys. Rev. B* **84**, 245114 (2011).
  - <sup>15</sup>U. Bovensiepen, *J. Phys.: Condens. Matter* **19**, 083201 (2007).
  - <sup>16</sup>D. E. Eastman and M. Kuznietz, *J. Appl. Phys.* **42**, 1396 (1971).
  - <sup>17</sup>L. Duo, M. Finazzi, and L. Braicovich, *Phys. Rev. B* **48**, 10728 (1993).
  - <sup>18</sup>F. Patthey, W.-D. Schneider, Y. Baer, and B. Delley, *Phys. Rev. Lett.* **58**, 2810 (1987).
  - <sup>19</sup>S.-K. Mo, W. S. Lee, F. Schmitt, Y. L. Chen, D. H. Lu, C. Capan, D. J. Kim, Z. Fisk, C.-Q. Zhang, Z. Hussain, and Z.-X. Shen, *Phys. Rev. B* **85**, 241103(R) (2012).
  - <sup>20</sup>D. V. Vyalikh, S. Danzenbächer, C. Krellner, K. Kummer, C. Geibel, Yu. Kucherenko, C. Laubschat, M. Shi, L. Patthey, R. Follath, and S. L. Molodtsov, *J. Electron Spectrosc. Relat. Phenom.* **181**, 70 (2010).
  - <sup>21</sup>A. Mönnich, J. Lange, M. Bauer, M. Aeschlimann, I. A. Nechaev, V. P. Zhukov, P. M. Echenique, and E. V. Chulkov, *Phys. Rev. B* **74**, 035102 (2006).
  - <sup>22</sup>V. P. Zhukov, E. V. Chulkov, P. M. Echenique, A. Marienfeld, M. Bauer, and M. Aeschlimann, *Phys. Rev. B* **76**, 193107 (2007).
  - <sup>23</sup>E. V. Chulkov, A. G. Borisov, J. P. Gauyacq, D. Sánchez-Portal, V. M. Silkin, V. P. Zhukov, and P. M. Echenique, *Chem. Rev.* **106**, 4160 (2006).
  - <sup>24</sup>W. Berthold, U. Höfer, P. Feulner, E. V. Chulkov, V. M. Silkin, and P. M. Echenique, *Phys. Rev. Lett.* **88**, 056805 (2002).
  - <sup>25</sup>E. Knoesel, A. Hotzel, and M. Wolf, *Phys. Rev. B* **57**, 12812 (1998).
  - <sup>26</sup>J. Cao, Y. Gao, R. J. D. Miller, H. E. Elsayed-Ali, and D. A. Mantell, *Phys. Rev. B* **56**, 1099 (1997).
  - <sup>27</sup>A. Marini and R. Del Sole, *Phys. Rev. Lett.* **91**, 176402 (2003).
  - <sup>28</sup>B. Gumhalter, P. Lazic, and N. Doslic, *Phys. Status Solidi B* **247**, 1907 (2010).
  - <sup>29</sup>F. Schmitt, P. S. Kirchmann, U. Bovensiepen, R. G. Moore, J.-H. Chu, D. H. Lu, L. Rettig, M. Wolf, I. R. Fisher, and Z.-X. Shen, *New J. Phys.* **13**, 063022 (2011).
  - <sup>30</sup>P. S. Kirchmann and U. Bovensiepen, *Phys. Rev. B* **78**, 035437 (2008).
  - <sup>31</sup>D. V. Vyalikh, S. Danzenbächer, A. N. Yaresko, M. Holder, Yu. Kucherenko, C. Laubschat, C. Krellner, Z. Hossain, C. Geibel, M. Shi, L. Patthey, and S. L. Molodtsov, *Phys. Rev. Lett.* **100**, 056402 (2008).